Research Article

THE IMPACTS OF ELECTRIC CHARGING STATIONS ON DISTRIBUTION POWER GRIDS UNDER DIFFERENT SIMULATIONS USING JELLYFISH SWARM ALGORITHM

Dao Trong TRAN[1,*], *Minh Phuc DUONG* [2]

[1]Division of MERLIN, Faculty of Electrical and Electronics Engineering, Ton Duc Thang University, Ho Chi Minh city, Vietnam
[2]Power System Optimization Research Group, Faculty of Electrical and Electronics Engineering, Ton Duc Thang University, Ho Chi Minh City, Vietnam

trantrongdao@tdtu.edu.vn, duongphucminh@tdtu.edu.vn

[*]Corresponding author: Dao Trong Tran; trantrongdao@tdtu.edu.vn

DOI: 10.15598/aeee.v23i1.250101

Article history: Received Jan 1, 2025; Revised Feb 14, 2025; Accepted Mar 06, 2025; Published Mar 31, 2025.

Abstract. *This research presents different implementations for placing electric charging stations (ECSs) in distribution power networks (DPNs) to achieve the best total active power loss (TAPL). Solar generators (SGs) are also used to alleviate the adverse effects resulting from the presence of ECSs in the networks in terms of power loss and voltage profile. Artificial hummingbird algorithm (AHA), Jellyfish swarm algorithms (JS), and Northern goshawk optimization (NGO) are executed to determine the best placement of ECSs and SGs in an IEEE 33-node network for reaching a minimum loss and satisfying all the related constraints. There are four cases conducted in the whole research. In the first case, JS outperforms both AHA and NGO by providing the highest stability throughout all the trial runs and fastest convergence speed to the optimal solution in the best runs. Besides, the quantitative comparison also consolidates the robustness and reliability of JS compared to others. Based on the surprising performance, JS is continuously reapplied to solve another three cases of the considered problem. Through those three cases with the application of JS, the TAPL values of four scenarios with different numbers of ECSs are evaluated. Specifically, the results achieved by JS indicate that the higher number of ECSs leads to a higher value of TAPL and a higher voltage drop. On the other hand, the simultaneous placement of SGs and ECSs can result in smaller fluctuations of the voltage profile and smaller TAPL. Thus, the optimization placement of ECSs and SGs is crucial to DPNs for economic and technical purposes.*

Keywords

Electric charging stations, distribution power networks, solar generators, total active power loss, voltage profile.

1. Introduction

Nowadays, global warming is one of the most concerning problems due to its negative effects, which can apparently be experienced all around the globe [1]. The main contribution to these negative effects is the significant increase in CO2 concentration produced by different modern activities, including diesel-based vehicles [2]. Moreover, due to the rapid growth of the world economy, the fleet of gasoline and diesel cars in large cities and countries has impressively grown, damaging the environment there [3]. In this circumstance, the shift to electric vehicles is acknowledged to be the affordable solution for reducing CO2 emissions and improving air quality in such hustling cities and places [4, 5]. The growth of the use of electric vehicles leads to a demand for electric charging stations (ECSs) con-

nected to the distribution power network (DPN) [6]. However, the placement of ECS in the DPNs also has some negative effects, such as power loss enlargement or voltage deregulation. Renewable power sources are then proposed to reduce voltage drop and power loss [7].

By thoroughly understanding the advantages and disadvantages of placing ECS in the DPN, many researchers have conducted their research to enhance the advantages of placing ECS while simultaneously trying to mitigate the negative impacts. Firstly, a general look at the impacts caused by having the ECSs in DPN is given in [6]. Next, the presence of ECSs in the DPN is evaluated regarding power demand, harmonics, voltage sag, and transformer power loss [8]. Then, [9] focuses on identifying and analysing the impact of ECSs on the reliability of the IEEE-33 bus test system. After that, the impact of ECSs on the DPN planning problems is assessed and evaluated in [10]. After that, the effects of having ECSs in a real DPN in a Latin American intermediate city are investigated [11]. Furthermore, the influences of ECSs on a residential distribution network in Bangladesh are also studied in [12]. Since all the problems and negative impacts caused by ECSs in DPN have been fully identified, a lot of papers have been proposed to partly mitigate all these downsides of ECSs, considering different aspects and orientations. For example, the authors in [13, 14] offered a method to solve the problem of increasing peak hours caused by the charging process of electric cars, which did not happen in the past when gasoline cars were in high demand. Moreover, the authors also argue that the increase in peak hours leads to overload status, which badly affects all electrical devices in the network, such as transformers and distribution lines. Besides the negative effects on the electrical devices, the fluctuation of voltage and current are focused on in [15, 16]. In [17], an optimization model is suggested to minimize the voltage stability index and evaluate the charging demand and the economy aspect while building ECSs in the IEEE-33 node. In [18], a multi-objective function has been formulated to minimize voltage deviation and power loss simultaneously. The authors in [19] addressed the inadequacy of building an uncontrolled number of ECSs on the grid, and then a cost model of ECS operation was built for different circumstances. After that, an optimization tool is applied to determine the optimal location of ECSs. In [20], the authors focused on shortening the capital of ECS while considering the voltage boundaries and reactive power loss of the whole system.

In practice, renewable energy generators (REGs), mostly solar generators (SGs) and capacitor banks (CBs), have been deployed independently or compounded to alleviate the negative impacts caused by ECS in the grid and also reduce the pressure on the transmission network. For example, CBs are combined with distributed generators (DGs) in [21] to optimize the reconfiguration of DPN based on the employment of a multi-objective function to reach different indices such as power loss, integrating level, and voltage stability in different scenarios. Next, the authors in [22] focused on maximizing the power supplied by solar generators by combining both the placement of ECSs and renewable energy generators in DPN to reduce the reliance on transmission power networks. Besides, CBs are also integrated into the IEEE-33 bus and 34-bus DPN together with ECS to lessen the power loss and maintain the reliability of DPN [23]. On top of that, the authors in [24] suggested that using the CB is one of the most efficient methods to handle the negative effects caused by the improper position of placing ECSs in the DPN. The author also added that geographical convenience is the top priority while establishing an ECS, not power flow optimization for DPN; therefore, using auxiliary engineering solutions is highly recommended to maintain the designed capability of the DPN. However, the combination of CBs, SGs, and DGs are simultaneously integrated with the DPN along the ECSs to maximize the efficiency, as conducted in [25]. Besides, the related modelling, simulation, and control methods in terms of operations and charging methods of EVs under different conditions, both in theory and practice, are highly essential to providing references and data analysis in the developing and testing phases [26, 27]. Additionally, the author in [28] presents the approach to solving the of transferring power the wireless charging technology and by enhancing the efficiency of the battery management system (BMS) on EVs [29]. On top of that, the battery is a crucial element in an EV, among others. Therefore, manufacturers and researchers also need an overview of the market for electric vehicle batteries [30].

By deeply understanding the positive effects brought by placing ECS combined with REGs to the distribution girds, this research applied three meta-heuristic algorithms including Artificial hummingbird algorithm (AHA) [31], jellyfish algorithm (JS) [32], and Northern goshawk optimization (NGO) [33] to optimize the placement of ECS in the given DPN to achieve the minimum value of the main objective function which is minimizing the total active power loss (TAPL). The three algorithms are proposed based on the simulation of living behaviours of different species in nature such as, hummingbird, jellyfish, and northern goshawk. Besides, those algorithms are also evaluated with various tests both in theorical and real-world problems and they have proven their capabilities while compared to other published previously. For AHA, specifically, when tested on the Multiple Disc Clutch Brake design problem, the algorithm demonstrated its superiority over several others, including Artificial Bee Colony (ABC), Teaching-Learning-Based

Optimization (TLBO), and Passing Vehicle Search (PVS). JS, on the other hand, exhibited high performance compared to various algorithms, such as Particle Swarm Optimization (PSO), its improved version (IPSO), and Enhanced Colliding Bodies Optimization (ECBO), when addressing the 582-bar tower optimal design problem. Lastly, NGO was also tested on different practical optimization problems, such as Pressure Vessel Design, Welded Beam Design, and Speed Reducer Design, during its development phase. The results obtained across these problems indicated that NGO outperforms the Whale Optimization Algorithm (WOA), Marine Predators Algorithm (MPA), Tunicate Swarm Algorithm (TSA), and others.

Compared to previous studies, the study has main novelties as follows:

- Apply three meta-heuristic algorithms, including AHA, JS, and NGO, to solve the given problem of optimizing the placement of ECSs and REGs in the given DPN.
- Propose different cases of optimizing REGs and ECSs: 1) The placement of ECSs is optimized in the first step, and then the placement of REGs is optimized in the second step, and 2) The placement of EGSs is optimized in the first step and then the placement of ECSs is optimized in the second step.
- Different penetration levels of ECSs are tested, and then the corresponding capacity of REGs is optimized.

After running the three algorithms for simulation cases in an IEEE 33-node system, the contributions of the study can be summarized as follows:

- JS is the most suitable algorithm among the three applied algorithms for the problem of optimally installing ECSs and REGs in distribution power grids.
- The use of high penetration levels of ECSs in distribution power grids leads to a high voltage drop and a high power loss. However, the use of REGs can improve the voltage and total power loss in the distribution system.
- The optimal placement of REGs in the first stage and the optimal placement of ECS in the next stage have a better voltage profile and a smaller power loss.

In addition to the Introduction, other sections of the research are structured as follows: Section 2 presents the mathematical model of the given problem in terms of the main objective function and the related constraints; Section 3 briefly introduces the applied algorithms; Section 4 provides the discussion on the results achieved by the applied algorithms on different cases; finally, Section 5 reveals the important conclusions of the whole research.

2. Problem formula

2.1. The main objective function

This study minimizes the value of active power loss in the distributed power network (DPN). The mathematical expression of the objection function is given as follows [14]:

$$Minimize \quad TAPL = \sum_{n=1}^{N_{DL}} R_n \times I_n^2 \tag{1}$$

where $TAPL$ is the total active power loss in the considered DPN; n is the distribution line n; N_{DL} is the number of distribution lines of the considered DPN; R_n and I_n are respectively the resistance and current values of the distribution line n.

2.2. The related constraints

1) The power balance constraints

These constraints mean that the total active and reactive power supplied by all the generating sources in the grid must equal the active and reactive power demanded by the end user and power loss. The mathematical expression of the constraints is given below [34]:

$$P_{SL} + \sum_{m=1}^{N_{SGs}} P_{SG,m} = P_{LD} + \sum_{i=1}^{N_{CS1}} PL_{1,i} + \sum_{j=1}^{N_{CS2}} PL_{2,j} + \sum_{k=1}^{N_{CS3}} PL_{3,k} + P_{loss} \tag{2}$$

and

$$Q_{SL} + \sum_{c=1}^{N_{CBs}} Q_{CB,c} = Q_{LD} + Q_{loss} \tag{3}$$

In Equations (2) and (3), P_{SL} and Q_{SL} are active and reactive power received from the transmission network at slack node; $PL_{1,i}$ is the power supplied by the i^{th} ECS level 1 with $i = 1 \ldots N_{CS1}$ and N_{CS1} is the number of ECS level 1 in grid; $PL_{2,j}$ is the power supplied by the j^{th} ECS level 2 with $j = 1 \ldots N_{CS2}$ and N_{CS2} is the number of ECS level 2 in grid; $PL_{3,k}$ is the power supplied by the k^{th} ECS level 3 with

$k = 1 \dots N_{CS3}$ and N_{CS3} is the number of ECS level 3 in grid; $P_{SG,m}$ is the power supplied by the SGs m, with $m = 1 \dots N_{SGs}$ and N_{SGs} is the number of the SGs in grid; $Q_{CB,c}$ is the reactive power supplied by c^{th} CB with $c = 1 \dots N_{CBs}$ and N_{CBs} is the number of capacitor banks; P_{LD} and Q_{LD} are active and reactive power demanded by load; finally, P_{Loss} and Q_{Loss} are respectively active and reactive power loss caused by the transmission process.

2) The operating constraints of capacitor banks (CBs) and solar generators (SGs)

Similar to other electrical devices, both CBs and SGs will work safely and effectively if their outputs are varied in the allowed ranges as described in [35]:

$$P_{SG,m}^{low} \leq P_{SG,m} \leq P_{SG,m}^{high} \tag{4}$$

$$Q_{CB,c}^{low} \leq Q_{CB,c} \leq Q_{CB,c}^{high} \tag{5}$$

where $P_{SG,m}^{low}$ and $P_{SG,m}^{high}$ are the lowest and highest value of active power generated by the m^{th} SG; $Q_{CB,c}^{low}$ and $Q_{CB,c}^{high}$ are the lowest and highest values of reactive power supplied by the c^{th} CB.

3) The constraints of voltage and current amplitude

The presence of CBs and SGs in the considered DPN leads to a variation of both voltage and current amplitude in the whole network. However, these values can only change within particular boundaries to ensure the stability and reliability of the network [36].

$$U_{nd}^{low} \leq U_{nd} \leq U_{nd}^{high} \tag{6}$$

$$I_n \leq I_n^{high} \tag{7}$$

where U_{nd}^{low} and U_{nd}^{high} are the lowest and highest value of voltage at the nd^{th} node; I_{nd}^{high} is the highest value of current allowed to sent through the distribution line n; U_{nd} is the voltage value at the nd^{th} node with $nd^{th} = 1 \dots N_{nd}$ and N_{nd} is the number of node in grid.

4) The constraints of electrical charging stations (ECSs)

This constraint means that only all the ECSs can be placed from node two onward on the system. Moreover, each node is allowed to place only one ECS. The formulation of the constraint is given as follows [35]:

$$2 \leq Po_{ECS-L1}, Po_{ECS-L2}, Po_{ECS-L3} \leq N_{nd} \tag{8}$$

$$Po_{ECS-L1} \neq Po_{ECS-L2} \neq Po_{ECS-L2} \tag{9}$$

where Po_{ECS-L1}, Po_{ECS-L2}, Po_{ECS-L3} are the position of the ECS level 1, 2, and 3 in the grid.

5) Constraint of position for placing CBs and SGs

Similar to EVSs, both CBs and SGs can be placed from node two onwards in the network, as described below [37]:

$$2 \leq Po_{SG,m}, Po_{CB,c} \leq N_{nd} \tag{10}$$

where $Po_{SG,m}$ and $Po_{CB,c}$ are the position of the SGs and CBs in the grid.

6) The constraints of SGs' power factor

SGs are supposed to have power factors in the range of 0.85 to 1.0. so, the optimal power factor is constrained within the range below:

$$PF_{SG,m}^{low} \leq PF_{SG,m} \leq PF_{SG,m}^{high} \tag{11}$$

where $P_{SG,m}^{low}$ and $PF_{SG,m}^{high}$ are the lower and upper limits of the m^{th} SG's power factor.

3. Applied methods

This section will briefly introduce the update mechanisms of the three applied algorithms for new solutions. Note that the update mechanism is critical in differentiating a particular meta-heuristic algorithm from many others.

3.1. The Artificial hummingbird algorithm (AHA)

The update method for new solutions of AHA is inspired by the variation on position of the hummingbird in its foraging process in nature. The update process is subsequently executed using three phases and their specific expressions will be given as follows [31]:

$$X_n^{new,P1} = X_{sl} + \varepsilon_1 \times NV \times (X_n - X_{sl}) \tag{12}$$

$$X_n^{new,P2} = X_n + \varepsilon_2 \times NV \times X_n \tag{13}$$

$$X_n^{new,P3} = HB_n + Rnd \times (HB_n - LB_n) \tag{14}$$

In the three equations above, $X_n^{new,P1}$, $X_n^{new,P2}$, and $X_n^{new,P3}$ are respectively the new position of the hummingbird n at each phase, respectively with $n = 1, \dots N_{Ps}$ and N_{Ps} is initial population size; X_{sl} is the random selected position in the search space; ε_1 and ε_2 are the amplying factors; NV is the navigating factor; HB_n and LB_n the highest and lowest boundaries of the search space; Rnd is the random number between 0 and 1.

3.2. The Jellyfish algorithm (JS)

As mentioned earlier, the development of JS is based on the living practices of jellyfish in nature, particularly their movement practices in the ocean. These movements are also the main idea of the update method for producing new solutions in the search process for the optimal solution. The particular expression of the update method of JS is given below [32]:

$$X_n^{new} = \begin{cases} X_n + mt \times Rnd \times (HB_n - LB_n) \\ X_n + ST \end{cases} \quad \text{with } n = 1 \dots N_{PS} \tag{15}$$

With

$$ST = Rnd \times DT \tag{16}$$

$$DT = \begin{cases} X_R - X_n & \text{if } F_R > F_{X_n} \\ X_n - X_R & \text{if } F_{X_n} < F_R \end{cases} \tag{17}$$

In Equations (15) – (17), X_n^{new} and X_n are the new updated position and the considered position belonged to the jellyfish n of the population; mt is the moving transition factor and according to the authors mt is set by 0.1 to optimize the searching ability of the algorithm; ST is the length of the jump step; DT is the direction term; X_R and F_R are respectively the random jellyfish selected from the initial population and its fitness value.

3.3. The Northern goshawk optimization (NGO)

Similar to AHA and JS, the update method for new NGO solutions is also developed by simulating the living practices of the northern goshawk, particularly the hunting behavior, which is separated into two phases. The mathematical expressions of each phase will be given as follows [33]:

$$X_n^{new,P1} = \begin{cases} X_n + AF_1(X_R - AF_2 \times X_n), & F_{X_R} < X_n \\ X_n + AF_1(X_n - X_R), & F_{X_R} \geq X_n \end{cases} \tag{18}$$

where $X_n^{new,P1}$ is the new position of the the northern n of the population with $n = 1, 2, \dots N_{Ps}$ and N_{Ps} is the initial population size; X_n the current position of the northern n; AF_1 and AF_2 are, respectively, the amplifying factors are their values is random generated between 0 and 1; X_R is the random selected position in the search space.

After the update process for new solutions in the first phase is completed, the update for new solution in the second phase is executed using the expression below [33]

$$X_n^{new,P1} = X_n + S_{PHA} \times (2 \times AF_1 - 1) \times X_n \tag{19}$$

With

$$S_{PHA} = 0.02 \left(1 - \frac{IT}{IT^{max}}\right) \tag{20}$$

In Equations (19) and (20), $X_n^{new,P1}$ is the new position of the northern n in phase 2; S_{PHA} is the acreage of the posible hunting area; IT and IT^{max} are, respectively, the current index of iteration and the maximum index of iteration.

4. Results

AHA, JS and NGO are implemented for the simulation and evaluation. Each algorithm is run fifty trials to collect the optimal solutions, the best and worst solutions with the smallest and highest power losses, the best run convergence characteristic and the mean convergence characteristic of all runs. The program of solving study case is coded in MATLAB on a computer with 2.6 GHz of CPU and 8GB of RAM. For each case, the population and iteration number are set to 30 and 100. The selection of the population and the maximum iteration number must be selected suitably for getting the most optimal solution and the simulation time is not long [38]. Besides, the three applied algorithms are executed for 50 trial runs for the best solution before all the comparisons take place. This section employs the original IEEE 33-node distribution power grid to investigate the installation of SGs and ECSs. The single-line diagram of the grid is plotted in Figure 1 [25]. Input data of the grid consisting of load demand at each node, resistance, and reactance of each line are taken from [25]. The total load demand is 213.41 kW [25]. In the study, we simulate three scenarios and four study cases for each scenario, including:

- Case 1: Optimize the placement of three SGs in the original grid.
- Case 2: Use results from Case 1 and continue optimize the placement of ECSs.
- Case 3: Optimize the placement of ESCs in the original grid.
- Case 4: Use results from Case 3 and continue to optimize thee SGs.

In Scenario 1, 1 Level-1 EVS, 1 Level-2 EVS and 1 Level-3 EVS are considered. In the scenarios 2 and 3, each EVS type has two and three stations, respectively. It is assumed that the Level-1 EVS can charge 1000 cars simulataneously and the station needs the supply

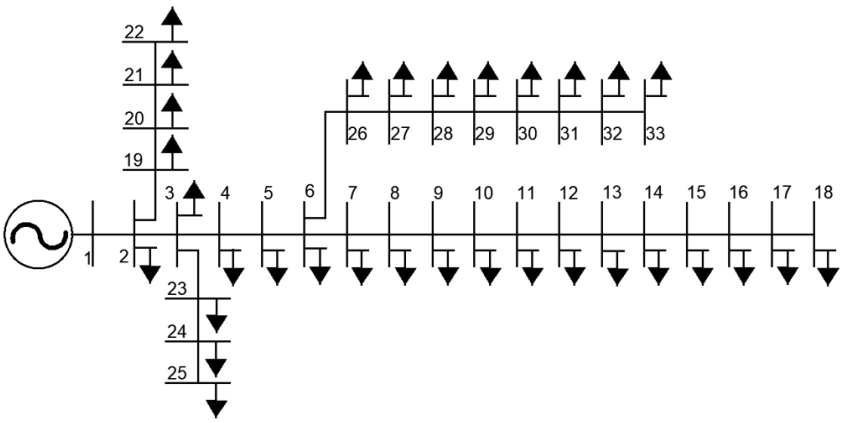

Fig. 1: The configuration of the IEEE 33-node system.

of 206.kW. Similarly, the car number and the capacity of Level-2 and Level-3 stations are 1000 cars and 435 kW, and 10 cars and 1,087 kW, respectively. The rated power of each charger is 1.9 kW in the Level-1 station, 4.0 kW in the Level-2 station and 100 kW in the Level-3 station [16]. The efficiency of each charger is selected to be 0.92.

4.1. Optimal placement of three SGs

The three curves in Figure 2a present the power loss of the trial runs and the summary of all trial runs, including the best, mean and worse loss, and standard deviation are given in Figure 2b. JS's power losses in red curve are less than those of NGO in black curve and AHA in green curve. The shortest bars of JS, NGO and AHA have the same loss of 14.52; however, JS reaches shorter maximum and mean loss bars than others. Furthermore, JS gets the smallest standard deviation (STD). In addition, the best run and mean run of fifty trials are given in Figure 3a and 3b. In Figure 3a, JS is faster than AHA and NGO from the fourtyth iteration to the eightyth iteration, then the three algorithms reach the same loss at the final iteration. In Figure 3b, the mean loss of NGO is always greater than that of AHA and JS. AHA can reach better mean loss values than JS for the first fourty iteration but then JS reaches better mean values than AHA for other iterations. Clearly, JS is faster and more stable than AHA and NGO.

In summary, the three algorithms could reach the same best solution but the mean solution and worst solutions from JS are less. JS reach faster and more stable convergence. Thus, JS is the most suitable algorithm for Case 1, and JS is selected for running other remaining cases.

Table 1 presents the optimal solutions achieved by JS in Case 1.

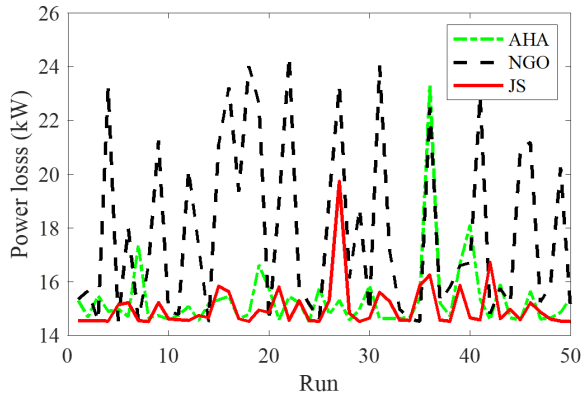

(a) Fifty optimal solutions

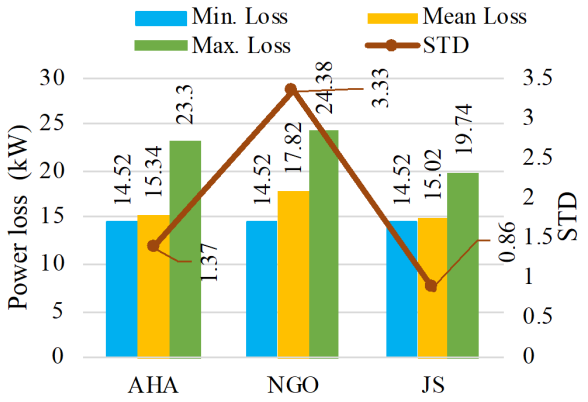

(b) Summary of results from fifty optimal solutions

Fig. 2: Results obtained by executed algorithms for Case 1.

4.2. Results obtained for all study cases

The results obtained for four cases of three scenarios by running JS are shown in Figure 4. Case 1 is the same for all scenarios, but Case 2, Case 3 and Case 4 are different in all scenarios. In general, the power

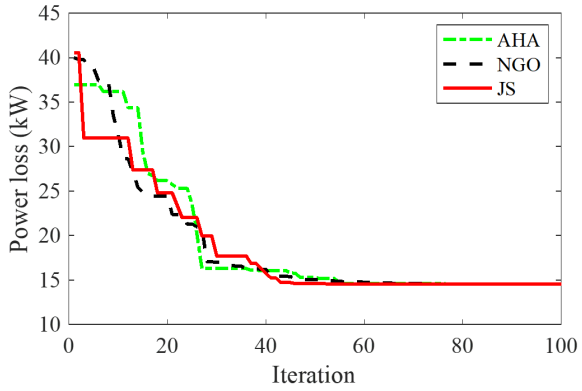

(a) The best run

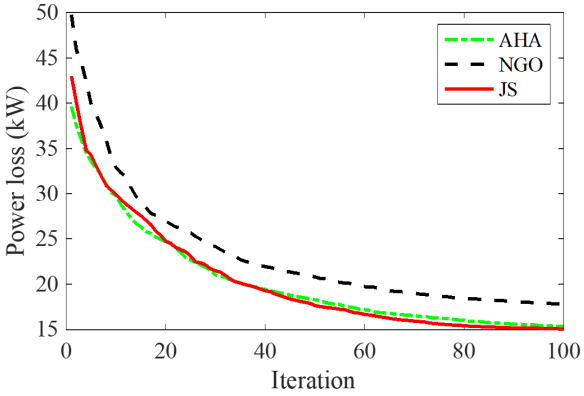

(b) The mean of all runs

Fig. 3: Comparison of convergence characteristics obtained by algorithms for Case 1.

loss is increased from Scenario 1 to Scenario 3. The losses are 17.858, 35.040, and 74.701 kW for Case 2 in Scenarios 1, 2 and 3, respectively. Similarly, the losses are 224.496, 270.355, and 357.126 kW for Case 3, and 20.832, 42.609, and 74.295 kW for Case 4, respectively. The results are obvious because the number of ECSs is increased from 3 to 6 and 9 in Scenarios 1, 2 and 3.

Among four study cases, Case 1 reach the smallest power loss because no ECSs but three SGs are placed in the grid. Case 3 suffers from the highest loss because load demand is greater due to the adding more ECSs and no SGs are placed. Case 2 and Case 4 had both

Tab. 1: The optimal solution achieved by the JS in Case 1.

Variables	Case 1
$Po_{SG,1}; P_{SG,1}$ (kW)	30; 1199.92
$Po_{SG,2}; P_{SG,2}$ (kW)	24; 1032.44
$Po_{SG,3}; P_{SG,3}$ (kW)	13; 753.55
$PF_{SG,1}$	0.85
$PF_{SG,2}$	0.87
$PF_{SG,3}$	0.86
Power loss (kW)	14.51576

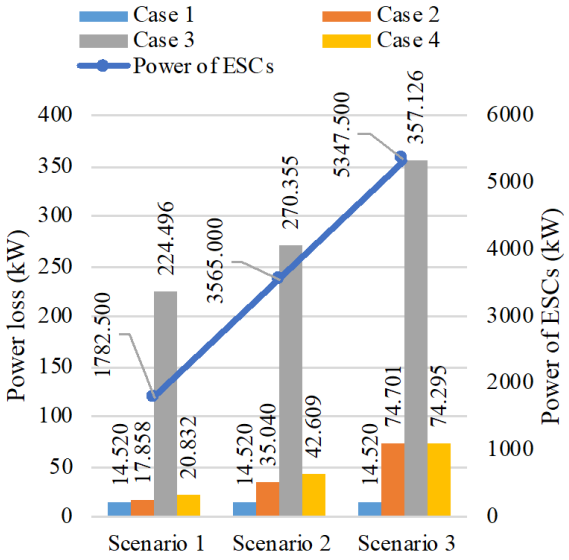

Fig. 4: Comparison of power loss for scenarios of Cases.

ECSs and SGs in the grid. However, Case 2 placed SGs first and ECS then but Case 4 placed ECSs first and SGs then. In Scenario 1, the loss is 17.858 kW for Case 2, and 20.832 kW for Case 4. In Scenario 2, the loss is 35.040 kW for Case 2, and 42.609 kW for Case 4. In Scenario 3, the loss is 74.701 kW for Case 2, and 74.295 kW for Case 4. Case 4 suffers a higher loss than Case 2 by about 3 kW in Scenario 1, 5.6 kW in Scenario 2. But Case 2 suffers a little higher loss than Case 4 by about 0.5 kW in Scenario 3.

The voltage profile of three scenarios of placing ECSs to the grid in Case 2 is presented in Figure 5. The figure clearly shows that the increase in the number of ECSs placed on the grid will lead to a higher voltage drop. Mainly, Scenario 3 resulted in the highest voltage drop, while Scenario 1 showed the smallest one among the three considered scenarios. Note that the voltage drop, in this case, is determined by optimizing the placement of SGs first at Case 1, and then ECSs are subsequently optimized.

Figure 6 shows the voltage profile in Case 3 with different scenarios of placing ECSs in the considered DPN. The degree of voltage drop at buses are completely huge compared to Case 2. Additionally, the placement of ECSs in Scenario 3 has violated the voltage limit described by the two red lines in the figure. Note that the placement of ECSs in three scenarios in this case is not supported by SG as seen in Case 2. Therefore, the presence of more ECSs will increase the load demand compared to the original configuration of the gird and also lead to another extensively voltage drop.

Case 4 is conducted with the additional placement of SGs to improve the voltage profile at all buses in Case

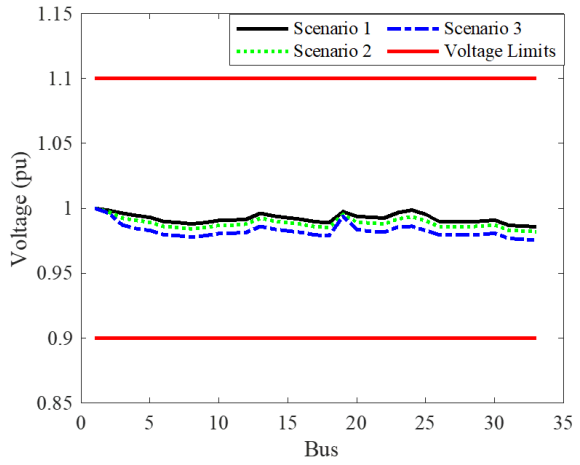

Fig. 5: Voltage profile of systems for different scenarios of Case 2 obtained by JS.

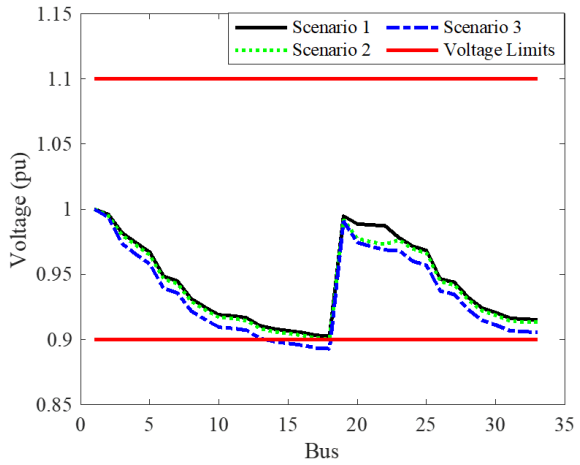

Fig. 6: Voltage profile of systems for different scenarios of Case 3 obtained by JS.

3, and the results are displayed in Figure 7. Moreover, of course, the placement of SGs in the grid is also optimized, besides the optimal position of ECSs executed in Case 3. The presence of SGs, in this case, has substantially improved voltage drop at all buses compared to Case 3. However, compared to Case 2, where the placement of SGs is first optimized, the fluctuation of voltage value in Case 4 is still more significant, especially at buses 19 to 25.

Tables 2, 3, and 4 present the optimal solutions achieved by JS in the three scenarios of the last three cases.

5. Conclusions

This paper applied three meta-heuristic algorithms to optimize the placement of SGs and ECSs in different cases for TAPL evaluation. The three algorithms are

Tab. 2: The optimal results obtained by JS in Scenario 1 of the last three cases.

Variable	Case 2	Case 3	Case 4
Po_{ECS-L1}	30	20	20
Po_{ECS-L2}	19	19	19
Po_{ECS-L3}	2	2	2
$Po_{SG,1}$; $P_{SG,1}$ (kW)	30; 1199.92	-	24; 1110.379
$Po_{SG,2}$; $P_{SG,2}$ (kW)	24; 1032.44	-	30; 1214.597
$Po_{SG,3}$; $P_{SG,3}$ (kW)	13; 753.55	-	13; 764.416
$PF_{SG,1}$	0.85	-	0.887
$PF_{SG,2}$	0.87	-	0.85
$PF_{SG,3}$	0.86	-	0.868
Power loss (kW)	17.858	224.496	20.832

Tab. 3: The optimal results obtained by JS in Scenario 2 of the last three cases.

Variable	Case 2	Case 3	Case 4
Po_{ECS-L1}	20; 30	22; 3	22; 3
Po_{ECS-L2}	23; 3	20; 21	20; 21
Po_{ECS-L3}	19; 2	19; 2	19; 2
$Po_{SG,1}$; $P_{SG,1}$ (kW)	30; 1199.92	-	12; 933.958
$Po_{SG,2}$; $P_{SG,2}$ (kW)	24; 1032.44	-	30; 1295.216
$Po_{SG,3}$; $P_{SG,3}$ (kW)	13; 753.55	-	21; 1450.431
$PF_{SG,1}$	0.85	-	0.873
$PF_{SG,2}$	0.8722	-	0.85
$PF_{SG,3}$	0.8635	-	0.95
Power loss (kW)	35.04	270.355	42.609

Tab. 4: The optimal results obtained by JS in Scenario 3 of the last three cases.

Variable	Case 2	Case 3	Case 4
Po_{ECS-L1}	21; 24; 30	4; 23; 24	4; 23; 24
Po_{ECS-L2}	4; 20; 23	20; 21; 22	20; 21; 22
Po_{ECS-L3}	2; 3; 19	2; 3; 19	2; 3; 19
$Po_{SG,1}$; $P_{SG,1}$ (kW)	30; 1199.92	-	30; 1279.705
$Po_{SG,2}$; $P_{SG,2}$ (kW)	24; 1032.44	-	24; 1914.165
$Po_{SG,3}$; $P_{SG,3}$ (kW)	13; 753.55	-	12; 948.250
$PF_{SG,1}$	0.85	-	0.85
$PF_{SG,2}$	0.8722	-	0.95
$PF_{SG,3}$	0.8635	-	0.893
Power loss (kW)	74.701	357.126	74.295

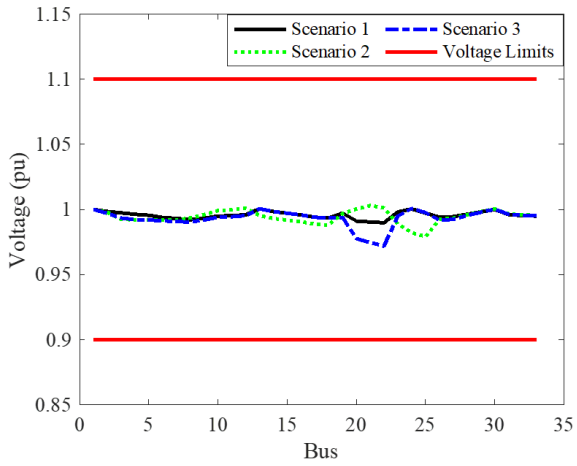

Fig. 7: Voltage profile of systems for different scenarios of Case 4 obtained by JS.

including the artificial hummingbird algorithm (AHA), the jellyfish algorithm (JS), and Northern goshawk optimization (NGO). These algorithms are executed on the IEEE 33-node for the first case to find out the best one. In the first case, JS outperformed two others in finding the optimal placement of SGs and reaching the best power loss value. Then, JS is used to investigate the TAPL value of the whole grid in the three remaining cases with the number of ECSs increasing from one to three for three scenario and the fixed number of SGs. The results from these scenarios indicate that the optimal placement of SGs to the grid before ECSs results in a better power loss value, except for Scenario 3, where the number of ECSs at all levels is three for each. Besides, the more ECSs integrated into the grid, the greater the power loss and the voltage drop. Additionally, several limitations remain that should be addressed to enhance the practicality and contribution of this work:

- The analysis is limited to the standard IEEE -node DPN configuration; a practical DPN should also be considered.
- Other objective functions, such as minimizing the total voltage deviation index, minimizing the power source, minimizing the energy cost, etc., should be evaluated.
- The study primarily focuses on solving the given problem from a planning perspective. The operational perspective should be explored.
- Given that solar generators (SGs) provide power only during daylight hours, energy storage systems (ESSs) should be integrated to compensate for nighttime shortages when SGs are inactive.
- The feasibility of SG and ESS placement sites should be evaluated, considering the geographic constraints of practical nodes.

Author Contributions

D. T. T. developed the applied methods, performed the simulation and results, and edited the final version of the manuscript. Both D. T. T. and M. P. D. contributed to the first draft of the manuscript and supervised the project.

References

[1] ABRAHMS, B., et al. Climate change as a global amplifier of human–wildlife conflict. *Nature Climate Change*. 2023, vol. 13, iss. 3, pp. 224–234. DOI: 10.1038/s41558-023-01608-5.

[2] HUANG, Y., N. UNGER, K. HARPER, C. HEYES. Global Climate and Human Health Effects of the Gasoline and Diesel Vehicle Fleets. *GeoHealth*. 2020, vol. 4, iss. 3. DOI: 10.1029/2019GH000240.

[3] CAMES, M., E. HELMERS. Critical evaluation of the European diesel car boom - global comparison, environmental effects and various national strategies. *Environmental Sciences Europe*. 2013, vol. 25, iss. 1, p. 15. DOI: 10.1186/2190-4715-25-15.

[4] SKERLOS, S. J., J. J. WINEBRAKE. Targeting plug-in hybrid electric vehicle policies to increase social benefits. *Energy Policy*. 2010, vol. 38, iss. 2, pp. 705–708. DOI: 10.1016/j.enpol.2009.11.014.

[5] DAI, Z., H. LIU, M.O. RODGERS, R. GUENSLER. Electric vehicle market potential and associated energy and emissions reduction benefits. *Applied Energy*. 2022, vol. 322. DOI: 10.1016/j.apenergy.2022.119295.

[6] AHMAD, F., et al. Optimal location of electric vehicle charging station and its impact on distribution network: A review. *Energy Reports*. 2022, vol. 8, pp. 2314–2333. DOI: 10.1016/j.egyr.2022.01.180.

[7] TRAN, H. V., A. V. TRUONG, T. M. PHAN, T. T. NGUYEN. Optimal placement and operation of soft open points, capacitors, and renewable distributed generators in distribution power networks to reduce total one-year energy loss. *Heliyon*. 2024, vol. 10, iss. 5. DOI: 10.1016/j.heliyon.2024.e26845.

[8] KARMAKER, A. K., S. ROY, M. R. AHMED. Analysis of the Impact of Electric Vehicle Charging Station on Power Quality Issues. *International Conference on Electrical, Computer and Communication Engineering (ECCE), Cox'sBazar, Bangladesh*. 2019. DOI: 10.1109/ECACE.2019.8679164.

[9] DEB, S., K. KALITA, P. MAHANTA. Impact of electric vehicle charging stations on reliability of distribution network. *International Conference on Technological Advancements in Power and Energy (TAP Energy), Kollam, India*. 2017, pp. 1-6. DOI: 10.1109/TAPENERGY.2017.8397272.

[10] DEB, S., K. KALITA, P. MAHANTA. 22 - Distribution Network planning considering the impact of Electric Vehicle charging station load. *Smart Power Distribution Systems*. 2019, p. 529–553. DOI: 10.1016/B978-0-12-812154-2.00022-5.

[11] GONZÁLEZ, L. G., E. SIAVICHAY, J. L. ESPINOZA. Impact of EV fast charging stations on the power distribution network of a Latin American intermediate city. *Renewable and Sustainable Energy Reviews*. 2019, vol. 107, pp. 309–318. DOI: 10.1016/j.rser.2019.03.017.

[12] NAFI, I. M., S. TABASSUM, Q. R. HASSAN, F. ABID. Effect of Electric Vehicle Fast Charging Station on Residential Distribution Network in Bangladesh. *5th International Conference on Electrical Engineering and Information Communication Technology (ICEEICT), Dhaka, Bangladesh*. 2021, pp. 1-5. DOI: 10.1109/ICEEICT53905.2021.9667870.

[13] MASOUM, A. S., et al. Smart load management of plug-in electric vehicles in distribution and residential networks with charging stations for peak shaving and loss minimisation considering voltage regulation. *IET Generation, Transmission & Distribution* . 2011, vol. 5, iss. 8. DOI: 10.1049/iet-gtd.2010.0574.

[14] SORTOMME, E., M. M. HINDI, S. D. J. MACPHERSON, S. S. VENKATA. Coordinated Charging of Plug-In Hybrid Electric Vehicles to Minimize Distribution System Losses. *IEEE Transactions on Smart Grid*. 2011, vol. 2, no. 1, pp. 198-205. DOI: 10.1109/TSG.2010.2090913.

[15] PRAKASH, K., et al. Bi-level planning and scheduling of electric vehicle charging stations for peak shaving and congestion management in low voltage distribution networks. *Computers and Electrical Engineering*. 2022, vol. 102. DOI: 10.1016/j.compeleceng.2022.108235.

[16] SHAHIDINEJAD, S., S. FILIZADEH, E. BIBEAU. Profile of Charging Load on the Grid Due to Plug-in Vehicles. *IEEE Transactions on Smart Grid*. 2012, vol. 3, no. 1, pp. 135-141. DOI: 10.1109/TSG.2011.2165227.

[17] CHENG, S., P.-F. GAO. Optimal allocation of charging stations for electric vehicles in the distribution system. *3rd International Conference on Intelligent Green Building and Smart Grid (IGBSG), Yilan, Taiwan*. 2018, pp. 1-5. DOI: 10.1109/IGBSG.2018.8393550.

[18] KHALKHALI, K., et al. Application of data envelopment analysis theorem in plug-in hybrid electric vehicle charging station planning. *IET Generation, Transmission & Distribution*. 2015, vol. 9, iss. 7, pp. 666–676. DOI: 10.1049/iet-gtd.2014.0554.

[19] ZHOU, G., Z. ZHU, S. LUO. Location optimization of electric vehicle charging stations: Based on cost model and genetic algorithm. *Energy*. 2022, vol. 247. DOI: 10.1016/j.energy.2022.123437.

[20] CHEN, L., C. XU, H. SONG, K. JERMSITTIPARSERT. Optimal sizing and sitting of EVCS in the distribution system using metaheuristics: A case study. *Energy Reports*. 2021, vol. 7, pp. 208–217. DOI: 10.1016/j.egyr.2020.12.032.

[21] MOHANTY, A. K., S. B. PERLI. Fuzzy Based Optimal Network Reconfiguration of Distribution System with Electric Vehicle Charging Stations, Distributed Generation, and Shunt Capacitors. *Advances in Electrical and Electronic Engineering*. 2023, vol. 21, iss. 2, pp. 81–91. DOI: 10.15598/aeee.v21i2.4599.

[22] PATEL, A. Solar heater-assisted electric vehicle charging stations: a green energy solution. *Hangkong Cailiao Xuebao/Journal of Aeronautical Materials*. 2023, vol. 43, pp. 520–534.

[23] BILAL, M., M. RIZWAN. Integration of electric vehicle charging stations and capacitors in distribution systems with vehicle-to-grid facility. *Energy Sources, Part A: Recovery, Utilization, and Environmental Effects*. 2021, pp. 1–30. DOI: 10.1080/15567036.2021.1923870.

[24] BILAL, M., A. KUMAR, M. RIZWAN. Coordinated Allocation of Electric Vehicle Charging Stations and Capacitors in Distribution Network. *IEEE 2nd International Conference On Electrical Power and Energy Systems (ICEPES), Bhopal, India*. 2021, pp. 1-6. DOI: 10.1109/ICEPES52894.2021.9699775.

[25] RAJESWARAN, S., K. NAGAPPAN. Optimum Simultaneous Allocation of Renewable Energy DG

and Capacitor Banks in Radial Distribution Network. *Circuits and Systems*. 2016, vol. 7, iss. 11, pp. 3556-3564. DOI: 10.4236/cs.2016.711302.

[26] MOHAMMADI, F., G.-A. NAZRI, M. SAIF. Modeling, Simulation, and Analysis of Hybrid Electric Vehicle Using MATLAB/Simulink. *International Conference on Power Generation Systems and Renewable Energy Technologies (PGSRET), Istanbul, Turkey*. 2019, pp. 1-5. DOI: 10.1109/PGSRET.2019.8882686.

[27] MOHAMMADI, F., G.-A. NAZRI, M. SAIF. A Bidirectional Power Charging Control Strategy for Plug-in Hybrid Electric Vehicles. *Sustainability*. 2019, vol. 11, no. 16. DOI: 10.3390/su11164317.

[28] ZHENG, J, C. JETTANASEN. Analysis of mutual inductance between transmitter and receiver coils in Wireless Power Transfer System of Electric Vehicle. *Advances in Electrical and Electronic Engineering*. 2023, vol. 21, no. 3, pp. 144-156. DOI: 10.15598/aeee.v21i3.4991.

[29] MOHAMMADI, F. Lithium-ion battery State-of-Charge estimation based on an improved Coulomb-Counting algorithm and uncertainty evaluation. *Journal of Energy Storage*. 2022, vol. 48. DOI: 10.1016/j.est.2022.104061.

[30] MOHAMMADI, F., M. SAIF. A comprehensive overview of electric vehicle batteries market. *e-Prime - Advances in Electrical Engineering, Electronics and Energy*. 2023, vol. 3. DOI: 10.1016/j.prime.2023.100127.

[31] ZHAO, W., L. WANG, S. MIRJALILI. Artificial hummingbird algorithm: A new bio-inspired optimizer with its engineering applications. *Computer Methods in Applied Mechanics and Engineering*. 2022, vol. 388. DOI: 10.1016/j.cma.2021.114194.

[32] CHOU, J.-S, D.-N. TRUONG. A novel metaheuristic optimizer inspired by behavior of jellyfish in ocean. *Applied Mathematics and Computation*. 2021, vol. 389. DOI: 10.1016/j.amc.2020.125535.

[33] DEHGHANI, M., S. HUBALOVSKY, P. TROJOVSKY. Northern Goshawk Optimization: A New Swarm-Based Algorithm for Solving Optimization Problems. *IEEE Access*. 2021, vol. 9, pp. 162059-162080. DOI: 10.1109/ACCESS.2021.3133286.

[34] DUONG, M. Q., et al. Determination of Optimal Location and Sizing of Solar Photovoltaic Distribution Generation Units in Radial Distribution Systems. *Energies*. 2019, vol. 12, no. 1. DOI: 10.3390/en12010174.

[35] DUONG, M. P., et al. Economic and Technical Aspects of Power Grids with Electric Vehicle Charge Stations, Sustainable Energies, and Compensators. *Sustainability*. 2025, vol. 17. DOI: 10.3390/su17010376.

[36] QI, Q., J. WU, C. LONG. Multi-objective operation optimization of an electrical distribution network with soft open point. *Applied Energy*. 2017, vol. 208, pp. 734–744. DOI: 10.1016/j.apenergy.2017.09.075.

[37] KIEN, L. C., T. T. NGUYEN, T. M. PHAN, T. T. NGUYEN. A study on the placement of photovoltaic units in the North and South of Vietnam for energy loss reduction by using a proposed slime mould algorithm. *Neural Computing and Applications*. 2023, vol. 35, iss. 31, pp. 23225–23247. DOI: 10.1007/s00521-023-08982-3.

[38] NGUYEN, T. T., D. N. VO, H. VAN TRAN, L. V. DAI. Optimal Dispatch of Reactive Power Using Modified Stochastic Fractal Search Algorithm. *Complexity*. 2019, vol. 2019, iss. 1. DOI: 10.1155/2019/4670820.